Nuclear Export of the Yeast Hexokinase 2 Protein Requires the Xpo1 (Crm1)-dependent Pathway*

Rafael Peláez[1], **Pilar Herrero, and Fernando Moreno**[2]

From the Department of Biochemistry and Molecular Biology, University of Oviedo, 33006 Oviedo, Spain

Hexokinase 2 (Hxk2) from *Saccharomyces cerevisiae* was one of the first metabolic enzymes described as a multifunctional protein. Hxk2 has a double subcellular localization; it functions as a glycolytic enzyme in the cytoplasm and as a regulator of gene transcription of several Mig1-regulated genes in the nucleus. However, the mechanism by which Hxk2 enters and leaves the nucleus is still unknown. In low glucose conditions, Hxk2 is phosphorylated at serine 14, but how this phosphorylation may affect glucose signaling is also unknown at the moment. Here we report that the Hxk2 protein is an export substrate of the carrier protein Xpo1 (Crm1). We also show that the Hxk2 nuclear export and the binding of Hxk2 and Xpo1 involve two leucine-rich nuclear export signals (NES) located between leucine 23 and isoleucine 33 (NES1) and between leucine 310 and leucine 318 (NES2). We also show that the Hxk2 phosphorylation at serine 14 promotes Hxk2 export by facilitating the association of Hxk2 with Xpo1. Our study uncovers a new cargo for the Xpo1 yeast exportin and identifies Hxk2 phosphorylation at serine 14 as a regulatory mechanism that controls its nuclear exit in function of the glucose levels.

Transport of macromolecules across the nuclear envelope occurs through nuclear pore complexes, which are embedded between the inner and the outer nuclear membrane (1). Whereas the protein components of the nuclear pore complex are largely stationary within the pore, soluble transport factors can be freely exchanged between the nuclear and the cytoplasmic compartment. *Saccharomyces cerevisiae* has several importin β-related proteins that are nuclear transport receptors which bind sequences on their transport cargos. Among the importin-β family members, the Xpo1 (Crm1) carrier is the major nuclear export receptor in higher eukaryotes as well as in the yeast *S. cerevisiae*. Xpo1 is the receptor for proteins containing leucine-rich nuclear export signals (NES)[3] and directly binds to NES-containing substrates in the presence of Gsp1 (RanGTP-binding protein) (2–4). Upon complex formation in the nucleus between Gsp1(GTP), Xpo1, and the adequate substrate, the complex translocates across the nuclear pore complex. In the cytoplasm, the export complex is disassembled through the combined action of Yrb1 (Ran GTPase-binding protein) and Rna1 (GTPase-activating protein). Both Gsp1(GDP) and the empty Xpo1 receptor reenter the nucleus to participate in further rounds of transport (1, 5). Unlike Xpo1, the β-importin carrier Msn5 is not only involved in nuclear export but also participates in protein import. Among the Msn5 export cargos identified so far is the transcriptional repressor Mig1, a protein involved in the repression of several glucose-regulated genes (6, 7). Export of Mig1 by the Msn5 receptor is regulated by the glucose concentration in the culture medium. Glucose regulates Mig1 function by affecting its phosphorylation state, which is catalyzed by the Snf1 protein kinase (8). Phosphorylation alters the subcellular localization of Mig1, causing it to be nuclear when high glucose is present and cytoplasmic when glucose is absent from the culture medium (9, 10).

In *S. cerevisiae*, hexokinase 2 (Hxk2) shuttles in and out of the nucleus (11) and the cytoplasmic Hxk2 catalyzes glucose phosphorylation at C6 during growth in high glucose conditions, whereas the nuclear Hxk2 is involved in the glucose repression signaling of several Mig1-regulated genes. The relative abundance of Hxk2 in the nucleus is Mig1 and glucose-dependent. Recent data revealed that the mechanism of Hxk2 sequestration in the nucleus is based on direct Hxk2 interaction with Mig1. This interaction is mediated by a 1- amino acid motif located between lysine 6 and methionine 15 of Hxk2 and the serine 311 of Mig1 (9, 12, 13). These findings suggest that the main regulatory role of Hxk2 is caused by its interaction with Mig1 to generate a repressor complex located in the nucleus of *S. cerevisiae*. At high glucose, nuclear Hxk2 stabilizes the repressor complex by blocking Mig1 phosphorylation in serine 311 by Snf1 protein kinase (9, 12). At low glucose, Hxk2 is phosphorylated at serine 14 (14). How this phosphorylation, catalyzed by a still-unknown kinase, may affect glucose signaling is unknown at the moment. Because serine 14 is within the 10-amino acid motif of Hxk2 involved in Mig1 interaction, it was hypothesized that the phosphorylation state of this residue could regulate the Hxk2 signaling function. However, the available results did not allow validation of this idea (11, 15, 16).

The mechanism by which Hxk2 enters and leaves the nucleus is still unknown. Because Hxk2 is too large to translocate through the nuclear pore complex by diffusion, its transport across the nuclear envelope is likely to be a mediated process, which may depend on carrier proteins. In this study, we show that the Hxk2 protein is an export cargo of the carrier protein

[3] The abbreviations used are: NES, nuclear export signals; Hxk2, hexokinase 2; GST, glutathione S-transferase; GFP, green fluorescent protein; DAPI, 4′,6-diamino-2-phenylindole; HA, hemagglutinin; PBS, phosphate-buffered saline.

Xpo1 in *S. cerevisiae*. We also show that the binding of Hxk2 to Xpo1 involves two leucine-rich NES. Finally, we have investigated the effect of a point mutation at serine 14 of Hxk2 on its Xpo1-dependent nuclear exit and Xpo1-interacting activity. Our results allow us to suggest that phosphorylation of serine 14 favors Hxk2 interaction with Xpo1 and regulates Hxk2 nuclear exit.

EXPERIMENTAL PROCEDURES

Strains and Growth Conditions—The following *S. cerevisiae* strains were used in this study: W303-1A (*MATa ura3-52 trp1-289 leu2-3,112 his3-Δ1 ade2-1 can1-100*) (17), Y03694 (*Matα his3Δ1 leu2Δ0 met15Δ0 ura3Δ0 msn5::kanMX4*) (euroscarf), FMY388 (*MATα his3Δ1 ura3Δ0 leu2Δ0 met15Δ0 MIG1::GFP*) (18), containing a GFP-tagged *MIG1* open reading frame (ORF) at its chromosomal location, FMY303R-02 (*MATa ura3-52 trp1-289 his3-Δ1 ade2-1 can1-100 hxk2::LEU2 XPO1::HA*), containing a 3×HA-tagged *XPO1* ORF at its chromosomal location, DBY2052 (*MATα hxk1::LEU2 hxk2-202 ura3-52 leu2-3, 2-112 lys2-801 gal2*) (19), conditional xpo1-1 (*xpo1::LEU2 [pRS313 (CEN HIS3) xpo1-1]*) (20). All mutant strains utilized in this work were derived from wild-type strain W303-1A.

Escherichia coli—DH5α (*F Ø80dlacZ ΔM15 recA1 endA1 gyrA96 thi-1 hsdR17(r_k-r_k-) supE44 relA1 deoRΔ 99U169*) was the host bacterial strain for the recombinant plasmid constructions.

Yeast cells were grown in the following media: YEPD, high glucose (2% glucose, 2% peptone, and 1% yeast extract); YEPE, low glucose (0.05% glucose, 3% ethanol, 2% peptone, and 1% yeast extract); synthetic media containing the appropriate carbon source and lacking appropriate supplements to maintain selection for plasmids (2% glucose (SD), 2% galactose (SGal) or 3% ethanol and 0.05% glucose (SE), and 0.67% yeast nitrogen base without amino acids). Amino acids and other growth requirements were added at a final concentration of 20–150 μg/ml. The solid media contained 2% agar in addition to the components described above.

Plasmids—The yeast expression plasmids YEp352-HXK2, YEp352-HXK2/GFP, and YEp352-Mig1/GFP were constructed as indicated previously (12). To create *hxk2* mutant alleles Hxk2*nes1*(Ala) (L23A, I27A, F30A, and I33A), Hxk2*nes2*(Ala) (L310A, I313A, L316A, and L318A), and Hxk2*nes1,2*(Ala) (L23A, I27A, F30A, I33A, L310A, I313A, L316A, and L318A), plasmids YEp352-HXK2 and YEp352-HXK2/GFP were used as the template in conjunction with oligonucleotides HXK2-L23A/I27A/F30A/I33A-forward (-f) (CGATGTGCCAAAGG-AA<u>GCG</u>ATGCAACAA<u>GCT</u>GAGAAT<u>GCT</u>GAAAAA<u>GCT</u>-CTGTTCCAACTG), HXK2-L23A/I27A/F30A/I33A-reverse (-r) (CAGTTGGAACAGTGAA<u>AGC</u>TTTTT<u>C</u><u>AGC</u>ATTCT-C<u>AGC</u>TTGTTGCAT<u>CGC</u>TTCCTTTGGCACATCG), HXK2-L310A/I313A/L316A/L318A-f (TGTCTTCTGGTTACT-AC<u>GCA</u>GGTGAA<u>GC</u>TTTGCGT<u>GCG</u>GCC<u>GCG</u>ATGGAC-ATGTACAAACAAGG) and HXK2-L310A/I313A/L316A/L318A-r (CCTTGTTTGTACATGTCCAT<u>CGC</u>GGCC<u>CGC</u>A-CGCAA<u>AGC</u>TTCACC<u>TGC</u>GTAGTAACCAGAAGACA) in the PCR based site-directed mutagenesis method (21) (underlined letters represent nucleotide substitutions that gave rise

to mutations). The plasmids YEp352-HXK2ΔNES1/GFP and YEp352-HXK2ΔNES2/GFP were constructed by reverse PCR using the oligonucleotides Hxk2-NES1-f (GTTCAAGATC-TCCAACTGAAACTTTACAAGCCG), Hxk2-NES1-r (AGT-CAAGATCTCAATTCCTTTGGCACATCGGCC), Hxk2-NES2-f (ACGTACGCGTATGGACATGTACAAACAAG-GTT), and Hxk2-NES2-r (AACCACGCGTGTAGTAACCA-GAAGACATTTTTTC). Plasmid YEp352-HXK2ΔNES1,2/GFP was generated by cloning 990 bp of BstXI-Pst1 DNA fragment of YEp352-HXK2ΔNES2/GFP into the BstXI-Pst1 site of YEp352-HXK2ΔNES1/GFP plasmid. All nucleotide changes were verified by DNA sequencing.

GST fusion vector pGEX-HXK2 was constructed as indicated in Ahuatzi *et al.* (12). Plasmid pGEX-GSP1 for expression of GST-Gsp1 in *E. coli* was a gift from the E. Hurt laboratory (5), and plasmid pGEX-Xpo1 for expression of GST-Xpo1 in *E. coli* was a gift from C. N. Cole laboratory (22).

Fluorescence Microscopy—Yeast strains expressing the Hxk2-GFP, Mig1-GFP, Hxk2ΔNES1-GFP, Hxk2ΔNES2-GFP, Hxk2ΔNES1,2-GFP, Hxk2*nes1*(Ala)-GFP, Hxk2*nes2*(Ala)-GFP, Hxk2*nes1,2*(Ala)-GFP or Hxk2-S14A-GFP were grown to early log phase (A_{600} of less than 0.8) in synthetic high glucose medium (SD-ura). Half of the culture was shifted to synthetic low glucose medium (SE−ura) for 1 h. The media contained the appropriate carbon source and lacked the appropriate supplements to maintain selection of plasmids. Cells (25 μl) were loaded onto poly L-lysine-coated slides, and the remaining suspension was immediately withdrawn by aspiration. One microliter of DAPI (2.5 μg/ml in 80% glycerol) was added, and a covert slide was placed over the microscope slide. GFP and DAPI localization in live cultures was monitored by direct fluorescence using a Leica DM5000B microscope. To avoid the nonlinear range of fluorescent signals, cells highly overexpressing GFP-tagged fusion protein were excluded from further analyses. The localization of proteins was monitored by visual inspection of the images. At least 100 cells were scored in each of at least three independent experiments. The distribution of fluorescence was scored in the following way: *N* denotes a nuclear fluorescence signal; *C* denotes cytoplasmic fluorescence signal without nuclear fluorescence signal. Images representatives of the results obtained were shown. Images were processed in Adobe Photoshop CS.

Preparation of Crude Protein Extracts—Yeast protein extracts were prepared as follows. Yeasts were grown in 10–20 ml of synthetic high glucose medium (SD−ura) at 28 °C to an optical density at 600 nm of 0.8–1.0. Half of the culture was shifted to synthetic low glucose medium (SE−ura) for 1 h. Cells were collected, washed twice with 1 ml of 1 M sorbitol, and suspended in 100 μl of solubilization buffer (20 mM Hepes, pH 7.2, 100 mM potassium acetate, 2 mM magnesium acetate, 0.1% Tween 20, 10% glycerin). The cells were broken in the presence of glass beads by 1 pulse of 20 s at 6.0 m/s using a FastPrep homogenizer (Thermo Electron Co.), and 400 μl of the same buffer were added to the suspension. After centrifugation at 12,000 × *g* (9000 rpm) for 15 min at 4 °C, the supernatant was used as crude protein extract.

Enzyme Assay—Invertase activity was assayed in whole cells as previously described (23) and expressed as μmol of glucose released/min/100 mg of cells (dry weight).

Immunoblot Analysis—Mutant or wild-type yeast cells were grown to an optical density at 600 nm of 1.0 in selective medium containing high glucose (2%). The cells were collected by centrifugation (3000 $\times$ *g*, 4 °C, 2 min), and crude extracts were prepared as described above. For Western blotting, 20–40 μg of proteins were separated by SDS, 12% PAGE and transferred to enhanced chemiluminescence polyvinylidene difluoride transfer membrane (Amersham Biosciences) by electroblotting, which was then incubated with anti-Hxk2 antibody. Horseradish peroxidase-conjugated protein-A was used as secondary reactant. The complex was detected by the West Pico Chemiluminescent system (Pierce).

Coimmunoprecipitation Assay—Immunoprecipitation experiments were performed by using whole cell extracts from yeast strains with modified *XPO1* gene, which codes for a C-terminal Xpo1 protein tagged with 3HA epitopes and with or without the *HXK2* gene. The Δ*hxk2* mutant strain was transformed with the plasmids YEp352-HXK2ΔNES1,2 or YEp352-HXK2*nes1,2*(Ala). Extracts were incubated with anti-Hxk2 or anti-Pho4 polyclonal antibodies for 1 h at 4 °C. Protein A-Sepharose beads (Amersham Biosciences) were then added and incubated for 1 h at 4 °C. After extensive washes with Staph A buffer (150 mM NaCl, 100 mM Na_2HPO_4, 18 mM NaH_2PO_4, pH 7.3, 20% Triton X-100, 1% SDS, 5% deoxycholate), immunoprecipitated samples were boiled in SDS-loading buffer (50 mM Tris-HCl, pH 6.8, 100 mM dithiothreitol, 2% SDS, 0.1% bromphenol blue, 10% glycerol). The supernatant was subjected to 12% SDS, PAGE and detected by Western blot using anti-HA (Santa Cruz Biotechnology, Santa Cruz, CA) monoclonal antibody and horseradish peroxidase-conjugated protein-A by the West Pico Chemiluminescent system (Pierce). Experiments were performed a minimum of three times. Values shown are representative results from individual experiments.

GST Pulldown Experiments—GST fusion protein expression vector pGEX-XPO1 was transformed into *E. coli* strain BL21(DE3) pLysS. Cells were grown to A_{600} 0.5–0.8, induced with 0.5 mM isopropyl-1-thio-β-D-galactopyranoside at 37 °C for 3 h, and collected by centrifugation. The cell pellet was resuspended in PBS buffer (150 mM NaCl, 100 mM Na_2HPO_4, 18 mM NaH_2PO_4, pH 7.3) and sonicated. Insoluble material was removed by centrifugation (17,000 $\times$ *g* for 20 min at 4 °C). Soluble extract was incubated with glutathione-Sepharose 4B (Amersham Biosciences) for 1 h at 4 °C, washed extensively with PBS buffer, and resuspended in the same buffer. The Xpo1-GST fusion protein coupled to glutathione-Sepharose was incubated with yeast whole cell extracts from the wild-type yeast strain or cell extracts from a Δ*hxk2* mutant strain transformed with the plasmids YEp352-HXK2ΔNES1,2, YEp352-HXK2*nes1,2*(Ala), or YEp352-HXK2S14A for 1 h at 4 °C in PBS buffer. The cell extracts were obtained from yeast cells grown in SD medium containing high glucose (2%) and shifted to 0.05% glucose plus 3% ethanol (low glucose) for 1 h. Beads were gently washed 5 times with 2.5 ml of PBS buffer (150 mM NaCl, 100 mM Na_2HPO_4, 18 mM NaH_2PO_4, pH 7.3), boiled in 25 μl of sample-loading buffer, and analyzed by SDS-PAGE followed by West-

ern blot using anti-Hxk2 antibodies and horseradish peroxidase-conjugated protein A. Bound antibodies were detected using the West Pico Chemiluminescent system (Pierce).

GST fusion protein expression vectors pGEX-HXK2 and pGEX-GSP1 were transformed into *E. coli* strain BL21(DE3) pLysS. Cells were grown to A_{600} 0.5–0.8, induced with 0.5 mM isopropyl-1-thio-β-D-galactopyranoside at 37 °C for 3 h, and collected by centrifugation. Cell pellets were resuspended in PBS buffer and sonicated. The GST-Hxk2 and GST-Gsp1 fusion proteins coupled to glutathione-Sepharose beads were incubated with 2.5 units of thrombin (2 h at 4 °C) for site-specific separation of the GST affinity tag from Hxk2 and Gsp1 proteins. Affinity-purified Gsp1 was immediately loaded with GTP or GDP by adding 30 mM K_2PO_4 (pH 7.5), 1 mM GTP or 1 mM GDP, and 10 mM EDTA (pH 8.0), incubating at room temperature for 1 h, adding 20 mM magnesium acetate, incubating on ice for 30 min, and freezing at −80 °C. Gsp1-mediated Xpo1 interaction with Hxk2 was analyzed by incubating purified Hxk2 with GST-Xpo1 bound to glutathione-Sepharose beads in the presence of Gsp1(GTP) or Gsp1(GDP) for 1 h at 4 °C in PBS buffer. Beads were washed and analyzed as described above.

RESULTS

The Nuclear Exporter Msn5 Is Not Essential for Transporting Hxk2 to the Cytoplasm—At high glucose Hxk2 interacts with Mig1 to generate a glucose repressor complex in the nucleus. After glucose exhaustion, both Mig1 and Hxk2 translocate to the cytoplasm (9, 12). Msn5, an importin-β protein, is involved in the export of Mig1 from the nucleus to the cytoplasm in response to glucose removal (7). In contrast to the fairly well defined Mig1 export system (7), the mechanism underlying Hxk2 translocation to the cytoplasm upon glucose exhaustion is still unknown. We have tested the possible role of Msn5 in the export of Hxk2. Wild-type and Δ*msn5* mutant cells showed identical subcellular distribution of Hxk2 during growth at high or low glucose. Hxk2-GFP did not accumulate in the nucleus upon glucose exhaustion in the culture medium (Fig. 1, *A* and *B*). As a control experiment, we monitored the distribution of Mig1-GFP in both wild-type and Δ*msn5* mutant cells. In wild-type cells, the fluorescent Mig1-GFP protein shuttles between nucleus (high glucose) and cytoplasm (low glucose) (Fig. 1*A*), but in Δ*msn5* mutant cells, Mig1-GFP accumulates in the nuclei upon glucose removal (Fig. 1*B*) (7, 10). These results suggest that Hxk2 does not exit the nucleus as a complex with the Mig1 protein and support the idea that Msn5 does not play a major role in Hxk2-GFP nuclear export.

The Nuclear Exporter Xpo1 Is Essential for Transporting Hxk2 to the Cytoplasm—The carrier Xpo1 moves proteins from the nucleus to the cytoplasm by recognizing hydrophobic leucine rich NESs matching the consensus $\Phi X_{2-3} \Phi X_{2-3} \Phi X \Phi$ (where Φ is Leu, Ile, Val, Phe, or Met, and *X* indicates any amino acid residue) (1). Because Hxk2 presents two such motifs [23]LMQQIENFEKI[33] and [311]LGEILRLAL[319], we hypothesized that Xpo1 may mediate the nuclear export of Hxk2. To test this, we analyzed the subcellular localization of Hxk2-GFP in temperature-sensitive *xpo1-1* cells (20). The *xpo1-1* mutant cells were grown at the permissive temperature (25 °C) and then
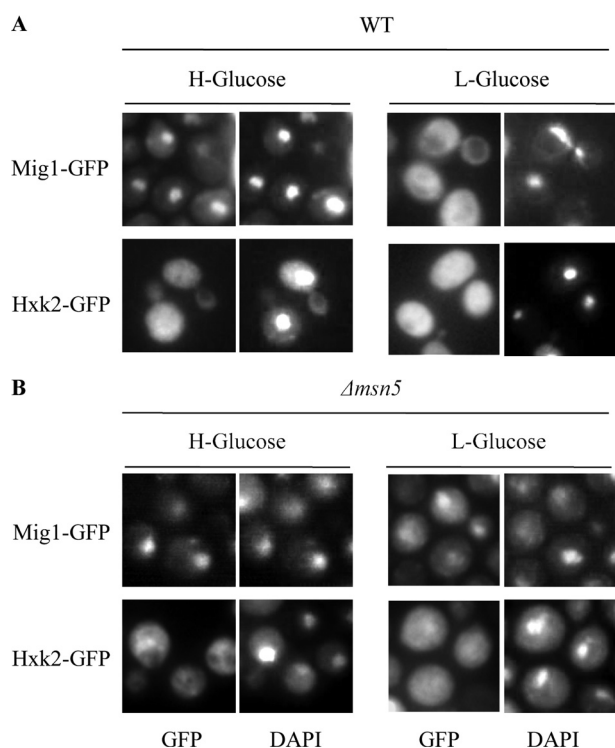
A

WT

H-Glucose   L-Glucose

Mig1-GFP

Hxk2-GFP

B

Δ*msn5*

H-Glucose   L-Glucose

Mig1-GFP

Hxk2-GFP

GFP   DAPI   GFP   DAPI

FIGURE 1. **Localization of Hxk2 and Mig1 in wild-type and Δ*msn5* yeast cells.** Yeast strain W303-1A (*WT*) (*A*) and Δ*msn5* mutant cells expressing Hxk2-GFP or Mig1-GFP from plasmids YEp352-HXK2/gfp and YEp352-MIG1/gfp respectively (*B*), were grown in high glucose synthetic medium (*H-Glucose*) until an $A_{600\ nm}$ of 1.0 was reached and then transferred to low glucose synthetic medium (*L-Glucose*) for 60 min. Cells were stained with DAPI and imaged for GFP and DAPI fluorescence.
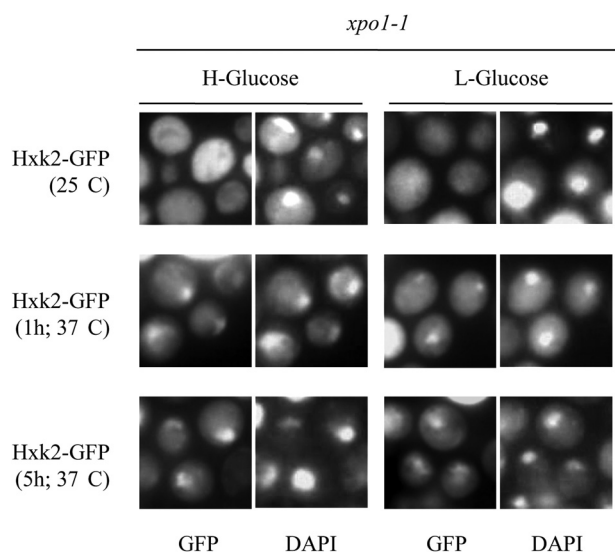
xpo1-1

H-Glucose   L-Glucose

Hxk2-GFP
(25 C)

Hxk2-GFP
(1h; 37 C)

Hxk2-GFP
(5h; 37 C)

GFP   DAPI   GFP   DAPI

FIGURE 2. **Nuclear export of Hxk2-GFP is inhibited in *xpo1-1* cells at the nonpermissive temperature.** The *xpo1-1* mutant cells expressing Hxk2-GFP from plasmid YEp352-HXK2/gfp were grown in high glucose synthetic medium (*H-Glucose*) until an $A_{600\ nm}$ of 1.0 was reached and then transferred to low glucose synthetic medium (*L-Glucose*). The cells were grown at 25 °C (permissive temperature) and then shifted to 37 °C (nonpermissive temperature) for 1 and 5 h. The localization of Hxk2-GFP was analyzed by fluorescence microscopy (GFP). Nuclear DNA was stained with DAPI.

shifted to 37 °C (nonpermissive temperature) for 1 and 5 h. No accumulation of Hxk2 was detected in the nuclei of *xpo1-1* cells grown at the permissive temperature (Fig. 2), and Hxk2 showed

identical subcellular distribution as in a wild-type strain (12) both in high and low glucose conditions (Fig. 2). However, in cells incubated at the nonpermissive temperature, an accumulation of Hxk2 in the nuclei was already observed after 1 h of culture in high and low glucose conditions (Fig. 2).

Mapping Residues Necessary for NES Function—We have determined whether the two putative NES sequences of Hxk2 are necessary for the exit of Hxk2 out of the nucleus. We, therefore, constructed three different strains in which *HXK2* was replaced by either *HXK2ΔNES1/GFP*, a mutant gene (*HXK2ΔL23I33*) with a 33-bp deletion between nucleotides +66 and +99, *HXK2ΔNES2/GFP*, a mutant gene (*HXK2ΔL310L318*) with a 27-bp deletion between nucleotides +927 and +954, or *HXK2ΔNES1,2/GFP*, containing both mutations. The analysis of intracellular localization of the different Hxk2 variants by fluorescent microscopy showed that Hxk2ΔNES1-GFP, Hxk2ΔNES2-GFP, and Hxk2ΔNES1,2-GFP were accumulated in the nuclei of Δ*hxk2* mutant cells carrying the respective mutant alleles (Fig. 3*A*). The ΔNES1, ΔNES2, and ΔNES1,2 mutations induced partial nuclear accumulation of Hxk2 in some, but not all, cells. The ΔNES1 mutation caused an export defect in ~50% of the cells. However, nuclear export of ΔNES2 was strongly defective with an export defect in ~72% of the cells. The nuclear accumulation of Hxk2ΔNES1,2 was as strong as the nuclear accumulation of Hxk2ΔNES2 mutant protein (Fig. 3*D*). Furthermore, Hxk2ΔNES1,2-GFP showed a nuclear accumulation in Δ*msn5* cells (Fig. 3*B*), indicating that Msn5 is not required for the import of Hxk2 from the cytoplasm to the nucleus. However, analysis of *in vivo* functionality of the truncated Hxk2ΔNES proteins reveals that, although expressed at a high level, none conferred the capacity to grow in glucose to a triple sugar kinase mutant strain (Δ*hxk1*Δ*hxk2*Δ*glk1*) (Fig. 3*E*) and did not restore the glucose repression capacity to a Δ*hxk1*Δ*hxk2* double mutant strain (Fig. 3*F*). These data suggest that the two NES sequences of the Hxk2 are required for efficient nuclear export *in vivo*, although the NES1 motif plays a minor role in the nuclear export of Hxk2 *in vivo*.

After this we performed a mutation analysis inside the NES sequences to delineate the Hxk2 NESs. The presence of regularly spaced hydrophobic amino acids such as leucine or isoleucine appears to be an important feature of the NES (24). Thus, we created three Hxk2-GFP mutants in which the four hydrophobic residues of NES1 and NES2 were replaced with alanine residues to generate Hxk2-L23A/I27A/F30A/I33A-GFP (Hxk2*nes1*(Ala)-GFP), Hxk2-L310A/I313A/L316A/L318A-GFP (Hxk2*nes2*(Ala)-GFP), and the double NES1,2 mutant (Hxk2*nes1,2*(Ala)-GFP). Cells expressing these mutant alleles showed nuclear accumulation of Hxk2-GFP (Fig. 3*C*). The *nes1*(Ala), *nes2*(Ala), and *nes1,2*(Ala) mutations induced partial nuclear accumulation of Hxk2 in some, but not all, cells. The *nes1*(Ala) and *nes2*(Ala) mutations caused an export defect respectively in 40 and 55% of the cells. However, nuclear export of *nes1,2*(Ala) double mutant was strongly defective with an export defect in 77% of the cells (Fig. 3*D*).

Furthermore, the Hxk2 *nes1,2*(Ala) mutant confers a partial glucose-grown capacity to a triple sugar kinase mutant strain (Δ*hxk1*Δ*hxk2*Δ*glk1*) (Fig. 3*E*) and also restores partial glucose
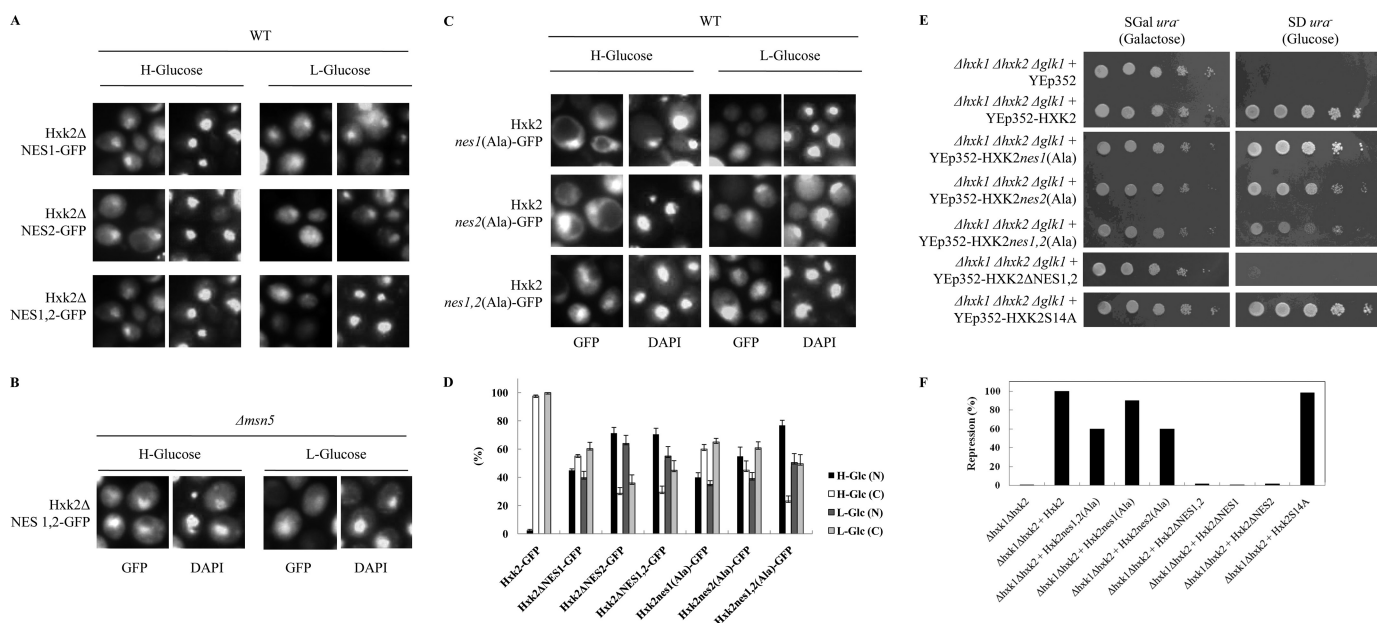
FIGURE 3. **Identification of Hxk2 NESs.** *A*, the Δ*hxk2* mutant strain was transformed with plasmids YEp352-HXK2ΔNES1/gfp, YEp352-HXK2ΔNES2/gfp, and YEp352-HXK2ΔNES1,2/gfp. The Δ*msn5* mutant strain was transformed with plasmid YEp352-HXK2ΔNES1,2/gfp (*B*), and the Δ*hxk2* mutant strain was transformed with plasmids YEp352-HXK2*nes1*(Ala)/gfp, YEp352-HXK2*nes2*(Ala)/gfp, and YEp352-HXK2*nes1,2*(Ala)/gfp (*C*). Transformed cells were grown in high glucose synthetic medium (*H-Glucose*) until an $A_{600\ nm}$ of 1.0 was reached and then transferred to low glucose synthetic medium (*L-Glucose*) for 60 min. The cells were visualized by fluorescence microscopy, and DAPI staining revealed nuclear DNA. *D*, the localization of fluorescent reporter proteins was determined in at least 100 cells in three independent experiments; *N* denotes a nuclear fluorescence signal; *C* denotes cytoplasmic fluorescence signal without nuclear fluorescence signal. Means and S.D. are shown for at least three independent experiments. *E*, the Δ*hxk1*Δ*hxk2*Δ*glk1* triple mutant strain was transformed with YEp352, YEp352-HXK2, YEp352-HXK2*nes1*(Ala), YEp352-HXK2*nes2*(Ala), YEp352-HXK2*nes1,2*(Ala), YEp352-HXK2ΔNES1,2, and YEp352-HXK2S14A plasmids and grown overnight in synthetic media with galactose as carbon source (*SGal ura⁻*). 5-Fold serial dilutions of a A_{600} 1.0 overnight culture were plated on SD *ura⁻* medium and photographed after 48h. *F*, the Δ*hxk1*Δ*hxk2* double mutant strain was transformed with YEp352, YEp352-HXK2, YEp352-HXK2*nes1,2*(Ala), YEp352-HXK2*nes1*(Ala), YEp352-HXK2*nes2*(Ala), YEp352-HXK2ΔNES1,2, and YEp352-HXK2S14A plasmids. Transformed cells were grown in high glucose synthetic medium until an $A_{600\ nm}$ of 1.0 was reached. Invertase activity was assayed in whole cells. Values are the averages of results obtained on four independent experiments. The average values have S.E. of 10% or less.

repression to a Δ*hxk1*Δ*hxk2* double mutant strain (Fig. 3*F*). Taken together, these results demonstrate that Leu-23, Ile-27, Phe-30, and Ile-33 are critical amino acid residues in the Hxk2 NES1 sequence, and Leu-310, Ile-313, Leu-316, and Leu-318 are critical amino acid residues in the Hxk2 NES2 sequence. Furthermore, because mutation of either NES sequence affects Hxk2 export, both NES sequences are essential for the nuclear export of Hxk2-GFP. Thus, a defect in both NES sequences increases the nuclear accumulation of Hxk2. These results are consistent with the idea that Xpo1 protein participates in Hxk2 nuclear export and prompted us to further define the possible role of this carrier in Hxk2 nuclear trafficking.

Hxk2 Interacts with the Xpo1 Exportin—To test whether Hxk2 binds to Xpo1 *in vivo* and *in vitro*, we have used an immunoprecipitation assay in cells expressing HA-Xpo1 as a fusion protein and Hxk2, Hxk2ΔNES1,2 or Hxk2*nes1,2*(Ala) as the only Hxk2 isoenzyme. Cell extracts from an Δ*hxk2* mutant strain transformed with plasmid YEp352-HXK2, YEp352-HXK2ΔNES1,2, or YEp352-HXK2*nes1,2*(Ala) were immunoprecipitated with an anti-Hxk2 antibody. The resulting immunoprecipitates were assayed for the presence of Xpo1-HA by immunoblot analysis with anti-HA antibodies. As shown in Fig. 4*A*, a specific signal of Xpo1 was observed only with samples immunoprecipitated with an anti-Hxk2 antibody in the strain expressing the wild-type Hxk2; no signals were observed when the experiment was done using the strain expressing the Hxk2ΔNES1,2 or Hxk2*nes1,2*(Ala) proteins, although as it can

be seen in Fig. 4*B*, *lane 2* and *3*, Hxk2ΔNES1,2 and Hxk2*nes1,2*(Ala) that proteins are recognized by the anti-Hxk2 antibody. Moreover, similar amounts of the different Hxk2 proteins were detected in these immunoprecipitates by immunoblot analysis with an anti-Hxk2 antibody (Fig. 4*A*). When an anti-Pho4 antibody or no antibody was used to detect unspecific immunoprecipitation and unspecific protein precipitation, respectively, no signals were observed. Thus, this interaction is dependent on the production of HA-tagged Xpo1 and the NESs of Hxk2 as well as an anti-Hxk2 antibody. Similarly, the Hxk2-Xpo1 interaction was also observed when the cell extracts were immunoprecipitated with an anti-HA antibody, and the resulting immunoprecipitates were assayed for the presence of Hxk2 by immunoblot analysis with anti-Hxk2 antibodies (data not shown).

To confirm the Xpo1-Hxk2 interaction, we performed GST pulldown experiments with crude protein extracts and purified GST-Xpo1 fusion protein produced from bacteria. As shown in Fig. 4*C*, a clear retention of Hxk2 protein was observed for the sample containing GST-Xpo1 and crude extract from the Δ*hxk2* mutant strain transformed with the YEp352-HXK2 plasmid. However, no retention of Hxk2ΔNES1,2 or Hxk2*nes1,2*(Ala) proteins was detected in the samples containing GST-Xpo1 and crude extract from the Δ*hxk2* strain transformed with plasmids YEp352-HXK2ΔNES1,2 or YEp352-HXK2*nes1,2*(Ala). When a control with GST protein in the reaction mixture was used, no signal was observed.
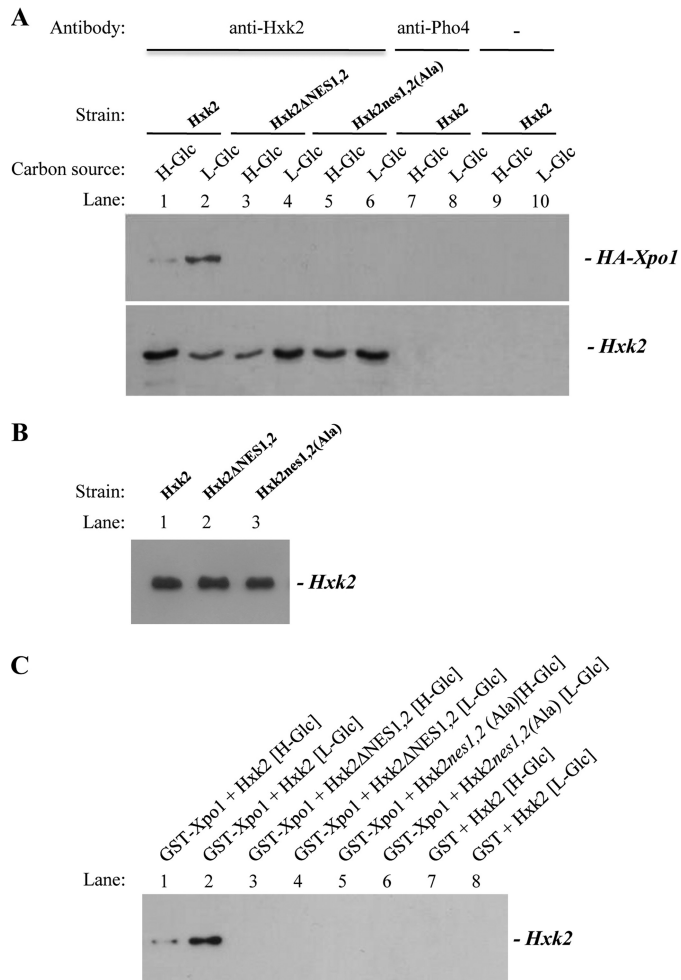
A

B

C

FIGURE 4. **Interaction of Hxk2 with Xpo1.** *A, in vivo* co-immunoprecipitation of HA-Xpo1 with Hxk2. Cell extracts from wild-type strain (*Hxk2*) and Δ*hxk2* mutant cells transformed with YEp352-HXK2ΔNES1,2 and YEp352-HXK2*nes1,2*(Ala) plasmids which express Hxk2ΔNES1,2 and Hxk2*nes1,2*(Ala) proteins, respectively, were immunoprecipitated with a polyclonal anti-Hxk2 antibody (*lanes 1–6*) or a polyclonal antibody to Pho4 (*lanes 7* and *8*). Cell extracts from the wild-type strain W3031A grown in SD (*H-glucose*) and SE (*L-glucose*) media were used as control (*lanes 9* and *10*). Immunoprecipitates were separated by 12% SDS-PAGE, and co-precipitated HA-Xpo1 was visualized on a Western blot with monoclonal anti-HA antibody. The level of immunoprecipitated Hxk2 in the blotted samples was determined by using anti-Hxk2 antibody. *B,* Western blot analysis of Hxk2, Hxk2ΔNES1,2, and Hxk2*nes1,2*(Ala) proteins with anti-Hxk2 antibody. *C,* GST pulldown assays of the interaction of Hxk2 with Xpo1. A GST-Xpo1 fusion protein was purified on glutathione-Sepharose columns. GST-Xpo1 was incubated with cell extracts from Δ*hxk2* mutant cells transformed with YEp352-HXK2, YEp352-HXK2ΔNES1,2, and YEp352-HXK2*nes1,2*(Ala) plasmids, which express Hxk2, Hxk2ΔNES1,2, and Hxk2*nes1,2*(Ala) proteins, respectively. The transformed strains were grown in high glucose (*H-Glc*) or low glucose medium (*L-Glc*). For the control samples GST protein was also incubated with the high Glc and low Glc cell extracts, but no signals were detected (*lanes 7* and *8*).

We conclude that consistent with the inability of NES mutants Hxk2ΔNES1,2 or Hxk2*nes1,2*(Ala) to exit the nucleus *in vivo* (Fig. 3, *A* and *C*), the mutants lacking the NES were unable to bind to the Xpo1 exportin (Fig. 4, *A* and *C*). These results also demonstrate that the Hxk2-Xpo1 interaction crucially depends on the identified NESs sequences of Hxk2. Moreover, because the interaction between the wild-type Hxk2 and HA-Xpo1 was systematically stronger with samples from low glucose-grown cultures than from high glucose cultures, our

data suggest that the low glucose condition increases the affinity of Hxk2 for the export receptor.

Formation of the Export Complex—In recent years a great deal of evidence has supported the idea that Xpo1 binds cooperatively to Gsp1(GTP) and its export cargo, leading to the formation of a trimeric transport complex in the nucleus (1). Once in the cytoplasm, GTP hydrolysis dissociates export complexes, thereby liberating cargo and the carrier, which can return to the nucleus for another round of export (25). Moreover, it has been suggested that the interaction of Xpo1 with NES-containing proteins can be regulated either positively or negatively by cargo phosphorylation (26, 27).

Because it could be thought that some unknown proteins in the extract could mediate the interaction between Hxk2 and Xpo1, we tried to show direct interaction of Xpo1 with Hxk2 using purified proteins in GST pulldown assays. We used both Hxk2 and GST-Xpo1 proteins purified from bacteria. First, we immobilized GST-Xpo1 on glutathione-Sepharose beads and analyzed binding of Hxk2 to these beads. Our results indicate that Hxk2 alone has a strong affinity for Xpo1 (Fig. 5*A, lane 2*). However, as expected for an exportin-type receptor, the complex formation between Xpo1 and Hxk2 is regulated by the guanine nucleotide-binding protein Gsp1. Our data in Fig. 5*A* indicate that Hxk2-Xpo1 complex is formed with equal readiness in the presence or absence of Gsp1(GTP) (*lane 4*). However, the presence of Gsp1(GDP) facilitates the dissociation of the complex between Hxk2 and Xpo1 (Fig. 5*A, lane 3*). This experiment suggests that a ternary complex between Xpo1, Gsp1, and Hxk2 is formed in a cooperative way *in vitro*. Moreover, the complex requires the GTP-bound state of Gsp1, because loading of Gsp1 with GDP disrupts the formation of the ternary complex.

On the other hand, it has been noted before that the phosphorylation of Hxk2 at serine 14 (28) happens when yeast cells grow in low glucose conditions (16). To examine whether there is a correlation between Hxk2 phosphorylation and an increased affinity for the export receptor, we generated a version of Hxk2-GFP with an alanine substitution at serine 14 (Hxk2-S14A-GFP). The fluorescent signals elicited by the Hxk2-S14A-GFP mutant cells show a mostly cytoplasmic distribution under high glucose conditions. However, the cells showed nuclear accumulation of Hxk2-S14A-GFP after a shift to low glucose conditions (Fig. 5*B*). The increase of nuclear signal is probably the consequence of a failure in Hxk2-Xpo1 interaction. This is because of the fact that when the Hxk2-S14A mutant was tested for its interaction, no significant signal was detected in the GST pulldown assay with GST-Xpo1 protein purified from bacteria and cell extracts obtained from high glucose grown cells. On the other hand, a very low signal was detected when we used cell extracts obtained from low glucose grown cells (Fig. 5*C*). As can be seen in Fig. 5*D*, the Hxk2-S14A protein is fully recognized by the anti-Hxk2 antibody. Furthermore, this Hxk2 mutant allele is fully functional, as it confers a glucose-grown capacity to a triple sugar kinase mutant strain (Δ*hxk1*Δ*hxk2*Δ*glk1*) (Fig. 3*D*) and restores glucose repression to a Δ*hxk1*Δ*hxk2* double mutant strain (Fig. 3*E*). Therefore, serine 14 phosphorylation of Hxk2 facilitates Hxk2-Xpo1 bind-

A

Lane: 1   2   3   4

- Hxk2

B

WT

H-Glucose   L-Glucose

Hxk2S14A-GFP

GFP   DAPI   GFP   DAPI

C

Lane: 1   2   3   4

- Hxk2

D

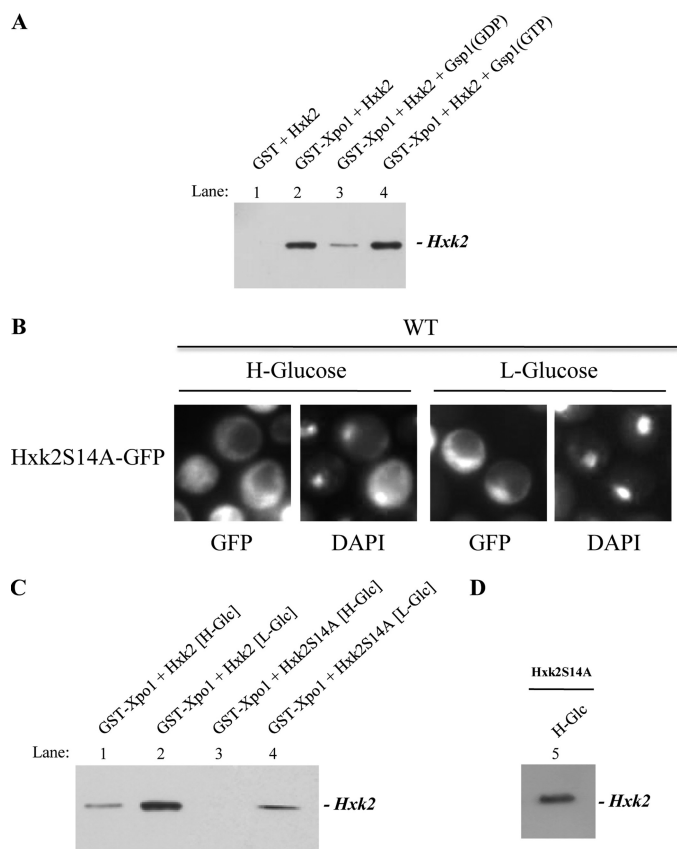Hxk2S14A

H-Glc

Lane: 5

- Hxk2

FIGURE 5. **The export Hxk2-Xpo1 complex formation.** *A*, GST pulldown assays of the effect of Gsp1 on the Hxk2-Xpo1 complex stability. GST-Hxk2 and GST-Gsp1 fusion proteins were purified on glutathione-Sepharose columns and incubated with thrombin to isolate, respectively, the Hxk2 and Gsp1 proteins. The Gsp1 protein was loaded with GTP to generate Gsp1(GTP) or with GDP to generate, Gsp1(GDP). The Hxk2 protein was incubated with purified GST-Xpo1 bound to glutathione-Sepharose beads in the presence of Gsp1(GTP) and Gsp1(GDP). The beads were washed extensively. Co-precipitated proteins were resolved by 12% SDS-PAGE and visualized on a Western blot with polyclonal anti-Hxk2 antibody. *B*, Hxk2-S14A-GFP fusion protein accumulates in the nucleus of Δ*hxk2* mutant cells transformed with the YEp352-HXK2S14A/gfp plasmid in low glucose conditions. Transformed cells were grown in high glucose synthetic medium (*H-Glucose*) until an $A_{600\ nm}$ of 1.0 was reached and then transferred to low glucose synthetic medium (*L-Glucose*) for 60 min. The cells were visualized by fluorescence microscopy and DAPI staining revealed nuclear DNA. *C*, GST pulldown assays of the interaction between Xpo1 and Hxk2-S14A. A GST-Xpo1 fusion protein was purified on glutathione-Sepharose columns. GST-Xpo1 was incubated with cell extracts from Δ*hxk2* mutant cells transformed with YEp352-HXK2 and YEp352-HXK2S14A and grown in high glucose (*H-Glc*) or low glucose (*L-Glc*) medium. The beads were washed extensively, and co-precipitated proteins were resolved by 12% SDS-PAGE and visualized on a Western blot with polyclonal anti-Hxk2 antibody. *D*, Western blot analysis of Hxk2-S14A protein with anti-Hxk2 antibody.

ing under conditions of high Gsp1(GTP) concentration, as would be expected in the nucleus of low glucose grown cells (1).

Taken together, these results demonstrate that Hxk2 interacts directly with Xpo1 *in vivo* and *in vitro* and that the NES1 ([23]LMQQIENFEKI[33]) and NES2 ([310]LGEILRLAL[318]) amino acids motives, identified as essential for nuclear exit of Hxk2, are also required for direct Hxk2-Xpo1 interaction. Moreover, a correlation between the phosphorylation state of Hxk2 and its nuclear exit rate could be suggested.

DISCUSSION

S. cerevisiae can distinguish between conditions of high and low glucose and adjust the expression levels of several genes

accordingly (29–31). Several of these changes are dependent on the Mig1 transcription factor and reflect modifications in the phosphorylation state of Mig1 catalyzed by Snf1 kinase (6) and modulated by nuclear Hxk2 (9). Previous evidence for nucleo-cytoplasmic shuttling of Hxk2 came from experiments with isolated nuclei and specific antibodies (11) or expressing an Hxk2-GFP fusion protein (12). The interaction between Hxk2 and Mig1 is required for Hxk2 to be retained within the nucleus, and upon overexpression of Mig1, an increase of nuclear Hxk2 is detected (9, 12). After glucose removal, Mig1 is exported to the cytoplasm and Msn5 importin directs Mig1 nuclear export (7, 10). Simultaneously, Hxk2 was no longer retained in the nucleus. Thus, Hxk2 shuttles between the nucleus and the cytoplasm in response to glucose availability, but the Hxk2 nuclear export mechanism is unknown.

In this study we have identified the Hxk2 protein as a substrate for the export receptor Xpo1 in *S. cerevisiae*. Hxk2 accumulates inside the nucleus of cells deficient in Xpo1 function and directly binds to Xpo1. The identification of Xpo1 as the nuclear export receptor for Hxk2 raises the question of the nature of the NES in Hxk2. Using GFP-tagged fusions of Hxk2-truncated proteins in two classical NES sequences (Hxk2ΔNES1, Hxk2ΔNES2, and Hxk2ΔNES1,2) or Hxk2 proteins mutated in four hydrophobic amino acids matching the consensus sequence of the two classical NESs (Hxk2*nes1*(Ala), Hxk2*nes2*(Ala), and Hxk2*nes1*,2(Ala)), we observed that a significant fraction of these mutant Hxk2 proteins were accumulated in the nucleus. Nuclear accumulation of Hxk2 was best detectable using the Hxk2*nes1*,2(Ala) mutants, whereas Hxk2*nes1*(Ala) and Hxk2*nes2*(Ala) mutants showed a weaker phenotype. The double Hxk2*nes1*,2(Ala) mutant displayed an increased nuclear accumulation (77%) in high glucose than in low glucose (50%) conditions. This result could be explained by the fact that in low glucose conditions the Mig1 protein is phosphorylated by the Snf1 kinase and translocates to the cytoplasm. Because the interaction between Hxk2 and Mig1 is required for Hxk2 to be retained within the nucleus, a weaker export defect was observed in low glucose-grown cells (9). Moreover, the *nes1*,2(Ala) mutant confers a partial glucose-grown capacity to a triple sugar kinase (Δ*hxk1*Δ*hxk2*Δ*glk1*) mutant strain and partially restores (62%) glucose repression to a double (Δ*hxk1*Δ*hxk2*) mutant strain. Therefore, the strain expressing the Hxk2*nes1*,2(Ala) mutant is to be chosen for studying Hxk2 export in living cells. Thus, we identified two functional NES sequences in the Hxk2 protein; a weaker NES1 (40% nuclear accumulation) and a stronger NES2 (55% nuclear accumulation), as has been demonstrated for other NES-cargo proteins (32). Because under high glucose conditions no obvious accumulation of Hxk2 in the nucleus was detected in a wild-type strain, our results also suggest that the rate of Hxk2 entry and exit to the nucleus is similar.

Several NES-cargo proteins transported by the exportin Xpo1 have been identified so far; however, only a few studies have showed which sequences within the transported protein mediated interaction, and rigorous evidence for a direct interaction between exportin and cargo is usually not provided. We demonstrate in this study that Hxk2 interacts directly with Xpo1 both at high and low glucose concentrations; however, a

strong signal was consistently detected in samples from cells grown in low glucose medium, and no interaction was observed between Xpo1 and the double Hxk2-NES1,2 mutant proteins in either high and low conditions. This indicates that the NESs motives are necessary for interaction between Xpo1 and Hxk2 and confirms that the Hxk2 protein is a cargo of Xpo1 in *S. cerevisiae*.

Our GST pulldown assay data suggest that the Hxk2-Xpo1 complex is stable in the presence of Gsp1(GTP) (Ran-GTP) protein, but is dissociated by Gsp1(GDP) binding. Thus, efficient dissociation of the Hxk2-Xpo1 complex is mediated primarily by Gsp1(GDP), which displaces Hxk2 from the Xpo1 protein.

It is well documented that Hxk2 is a phosphoprotein *in vivo*, pre-eminently labeled from ^{32}P inorganic phosphate after a shift of cells to medium with low glucose concentration. The only site of phosphorylation is the serine 14, as determined by mutation to alanine, which prevents phosphorylation *in vivo* (14, 16). Our finding that the Hxk2-S14A protein has a nuclear accumulation at low glucose conditions enabled us to correlate the phosphorylation state of Hxk2 with the intracellular distribution of the protein. Moreover, GST pulldown experiments show that the Hxk2-Xpo1 interaction is dramatically lost in Hxk2-S14A mutant cells grown under high glucose conditions and is severely diminished after a shift to low glucose conditions. The finding that nuclear export of Hxk2 requires the activating phosphorylation events is quite surprising because, although it has been suggested for a long time that the phosphorylation state of serine 14 could regulate the Hxk2 signaling function, the available results have not allowed validation of this idea until now (16, 33). Our data demonstrate that phosphorylation of serine 14 appears to act as a required switch that facilitates Hxk2 nuclear export in such a way that Hxk2 is predominantly cytoplasmic during growth in low glucose conditions (12).

In low glucose conditions, the Hxk2 interaction with Mig1 is abolished, and a transient increase in interaction between Snf1 and Mig1 was detected. These interaction patterns potentially stimulate Mig1 phosphorylation by Snf1 kinase and its Msn5-mediated nuclear exit, thereby relieving the transcriptional block of several glucose-regulated genes. Simultaneously, the Hxk2 protein is phosphorylated at serine 14 by an unknown protein kinase. We believe that phosphorylation of Hxk2 modulates its subcellular localization. We considered two possible models; (i) phosphorylation of nuclear Hxk2 increases its rate of nuclear export relative to nuclear import, and (ii) the phosphorylated cytoplasmic Hxk2 has low affinity for the import machinery, inhibiting Hxk2 nuclear import. The experimental data provided here support the first model because the phosphorylated Hxk2 has increased affinity to the Xpo1 receptor, and this fact could result in the increase in the export rate of Hxk2 after a shift to low glucose conditions.

However, our results do not clarify the nuclear import mechanism of Hxk2. At present, we can only demonstrate that nuclear import of Hxk2 is not mediated by the importin Msn5 because deletion of Msn5 does not abolish the import of Hxk2 to the nucleus. Although Mig1 interacts with Hxk2 in the nucleus, Mig1 does not need to form a complex with Hxk2 to enter the nucleus because Mig1 is found in the nucleus in a Δ*hxk2*Δ*snf1* double mutant (9, 34). Future studies will identify the factor(s) which facilitates Hxk2 nuclear import.

REFERENCES

1. Hutten, S., and Kehlenbach, R. H. (2007) *Trends Cell Biol.* **17,** 193–201
2. Maurer, P., Redd, M., Solsbacher, J., Bischoff, F. R., Greiner, M., Podtelejnikov, A. V., Mann, M., Stade, K., Weis, K., and Schlenstedt, G. (2001) *Mol. Biol. Cell* **12,** 539–549
3. la Cour, T., Gupta, R., Rapacki, K., Skriver, K., Poulsen, F. M., and Brunak, S. (2003) *Nucleic Acids Res.* **31,** 393–396
4. Kutay, U., and Güttinger, S. (2005) *Trends Cell Biol.* **15,** 121–124
5. Künzler, M., Gerstberger, T., Stutz, F., Bischoff, F. R., and Hurt, E. (2000) *Mol. Cell. Biol.* **20,** 4295–4308
6. Ostling, J., Carlberg, M., and Ronne, H. (1996) *Mol. Cell. Biol.* **16,** 753–761
7. DeVit, M. J., and Johnston, M. (1999) *Curr. Biol.* **9,** 1231–1241
8. Carlson, M. (1999) *Curr. Opin. Microbiol.* **2,** 202–207
9. Ahuatzi, D., Riera, A., Peláez, R., Herrero, P., and Moreno, F. (2007) *J. Biol. Chem.* **282,** 4485–4493
10. De Vit, M. J., Waddle, J. A., and Johnston, M. (1997) *Mol. Biol. Cell* **8,** 1603–1618
11. Randez-Gil, F., Herrero, P., Sanz, P., Prieto, J. A., and Moreno, F. (1998) *FEBS Lett.* **425,** 475–478
12. Ahuatzi, D., Herrero, P., de la Cera, T., and Moreno, F. (2004) *J. Biol. Chem.* **279,** 14440–14446
13. Moreno, F., Ahuatzi, D., Riera, A., Palomino, C. A., and Herrero, P. (2005) *Biochem. Soc. Trans.* **33,** 265–268
14. Kriegel, T. M., Rush, J., Vojtek, A. B., Clifton, D., and Fraenkel, D. G. (1994) *Biochemistry* **33,** 148–152
15. Mayordomo, I., and Sanz, P. (2001) *Yeast* **18,** 923–930
16. Randez-Gil, F., Sanz, P., Entian, K. D., and Prieto, J. A. (1998) *Mol. Cell. Biol.* **18,** 2940–2948
17. Wallis, J. W., Chrebet, G., Brodsky, G., Rolfe, M., and Rothstein, R. (1989) *Cell* **58,** 409–419
18. Riera, A., Ahuatzi, D., Herrero, P., Garcia-Gimeno, M. A., Sanz, P., and Moreno, F. (2008) *Biochem. J.* **415,** 233–239
19. Ma, H., and Botstein, D. (1986) *Mol. Cell. Biol.* **6,** 4046–4052
20. Stade, K., Ford, C. S., Guthrie, C., and Weis, K. (1997) *Cell* **90,** 1041–1050
21. Kadowaki, H., Kadowaki, T., Wondisford, F. E., and Taylor, S. I. (1989) *Gene* **76,** 161–166
22. Hammell, C. M., Gross, S., Zenklusen, D., Heath, C. V., Stutz, F., Moore, C., and Cole, C. N. (2002) *Mol. Cell. Biol.* **22,** 6441–6457
23. Gascón, S., and Lampen, J. O. (1968) *J. Biol. Chem.* **243,** 1567–1572
24. la Cour, T., Kiemer, L., Mølgaard, A., Gupta, R., Skriver, K., and Brunak, S. (2004) *Protein Eng. Des. Sel.* **17,** 527–536
25. Quan, X., Yu, J., Bussey, H., and Stochaj, U. (2007) *Biochim. Biophys. Acta* **1773,** 1052–1061
26. Benzeno, S., Lu, F., Guo, M., Barbash, O., Zhang, F., Herman, J. G., Klein, P. S., Rustgi, A., and Diehl, J. A. (2006) *Oncogene* **25,** 6291–6303
27. Sasaki, T., Kojima, H., Kishimoto, R., Ikeda, A., Kunimoto, H., and Nakajima, K. (2006) *Mol. Cell* **24,** 63–75
28. Heidrich, K., Otto, A., Behlke, J., Rush, J., Wenzel, K. W., and Kriegel, T. (1997) *Biochemistry* **36,** 1960–1964
29. Hedbacker, K., and Carlson, M. (2008) *Front. Biosci.* **13,** 2408–2420
30. Moreno, F., and Herrero, P. (2002) *FEMS Microbiol. Rev.* **26,** 83–90
31. Gancedo, J. M. (2008) *FEMS Microbiol. Rev.* **32,** 673–704
32. Neufeld, K. L., Nix, D. A., Bogerd, H., Kang, Y., Beckerle, M. C., Cullen, B. R., and White, R. L. (2000) *Proc. Natl. Acad. Sci. U.S.A.* **97,** 12085–12090
33. Herrero, P., Martínez-Campa, C., and Moreno, F. (1998) *FEBS Lett.* **434,** 71–76
34. Tomás-Cobos, L., and Sanz, P. (2002) *Biochem. J.* **368,** 657–663